Design and capabilities of a cluster implantation and deposition apparatus: first results on hillock formation under energetic cluster ion bombardment

Popok, Vladimir; Prasalovich, S.; Campbell, Eleanor E.B.

Published in:
Review of Scientific Instruments

Publication date:
2002

Document Version
Publisher's PDF, also known as Version of record

Design and capabilities of a cluster implantation and deposition apparatus: First results on hillock formation under energetic cluster ion bombardment

V. N. Popok,[a] S. V. Prasalovich, M. Samuelsson, and E. E. B. Campbell
Department of Experimental Physics, Gothenburg University and Chalmers University of Technology, 41296 Gothenburg, Sweden

(Received 15 July 2002; accepted 5 September 2002)

A description, advantages, and capabilities of a cluster implantation and deposition apparatus supplied by a pulsed cluster source from gaseous precursors are presented. A number of possible *in situ* and *ex situ* experimental methods to study cluster–surface collisions and modified substrate surfaces are discussed. Test experiments on cluster production show formation of Ar, N_2, and O_2 clusters with size up to 150 atoms for Ar and 60–70 molecules for the other gases. The possibility of cluster mass selection and acceleration up to 25 keV is reported. Nanosize hillock formation was found as a result of cluster–surface collisions with pyrolytic graphite and indium–tin–oxide. It is suggested that the hillocks' parameters such as size and density per surface area can be controlled by varying the implantation parameters and substrate material and thus provide a promising technique for nanoscale surface modification. © *2002 American Institute of Physics.*
[DOI: 10.1063/1.1518790]

I. INTRODUCTION

In the last few years there has been a growing interest in using cluster beams. It is motivated by demands to synthesize materials and to expand the existing technological possibilities where ion beams have almost reached their intrinsic limits.[1,2] Ionized cluster beams are a powerful and versatile tool for the modification of materials and processing of surfaces as an alternative to atomic ion techniques. With clusters consisting of up to a few thousand atoms it is possible to transport a large amount of material with just a single charge, thus greatly minimizing space-charge effects and charging of the target. Compared to ions, clusters generate multicollision effects with low energies at high densities that minimize radiation damage and channelling. By cluster assembling it is possible to produce materials with different properties and to control surface parameters. The properties of clusters depend on the number of constituent atoms or molecules. By controlling the size and structure of a cluster one can change electronic, optical, and chemical parameters of both the agglomerate and synthesized material. Many groups have studied the properties of free clusters in molecular beams and reviews of results have been presented, for example, in Refs. 3 and 4. Investigations of atom–cluster and cluster–cluster collisions have been performed as well.[5–7] The use of cluster ion beams for shallow implantation, dry etching, surface cleaning, smoothing, and thin film growth has been pioneered by the Kyoto group.[8–10]

However, the interaction of accelerated clusters with a substrate has not been studied in detail so far. There are many fundamental physical aspects that have to be investigated to provide successful production of materials with the required parameters using cluster assembling. In particular, clusters formed from gaseous precursors are interesting from the point of view of the dynamics of cluster ion impact on surfaces, the onset of nonadiabatic effects, and nonstationary quantum phase transitions.[11] They are also of interest for some applications. For instance, system-on-a-chip devices require triple gate oxide thicknesses. One method that has recently been reported to achieve this is through implanting various species of O, F, or Ar to enhance or N to retard the silicon oxidation rate.[12] The most advanced devices today use oxynitride gate dielectrics, however, new manufacturing processes will be needed when dimensions are reduced below 100 nm due to problems with chemical vapor deposition and thermal processing including nitrided oxides and metal oxides.[13] A promising alternative method is gate material modification through implanting controlled amounts of selected impurities into high-quality thin oxides. Thin oxides of a few nm thickness will require very low-energy implants in the 100–500 eV range. This is not possible with traditional ion implantation but may be feasible with cluster ion implantation. Oxygen cluster deposition can also be used for formation of thin SiO_2 insulating layers,[14,15] and has potential to be used for example in multilayered metal–oxide–semiconductor devices, or for growth of indium–tin–oxide (ITO) films.[16] Ar cluster bombardment provides a technological procedure for surface cleaning and smoothing with extremely low roughness inaccessible by ordinary ion techniques.[10] Very recently nanosize hillock formation on a Si surface under low-energy (tens keV) CO_2 cluster bombardment was reported.[17,18] By understanding the nature of the effect and controlling the cluster beam parameters, uniform structures with variable size and shape can be grown for various practical applications.

[a]Author to whom correspondence should be addressed; electronic mail: popok@fy.chalmers.se

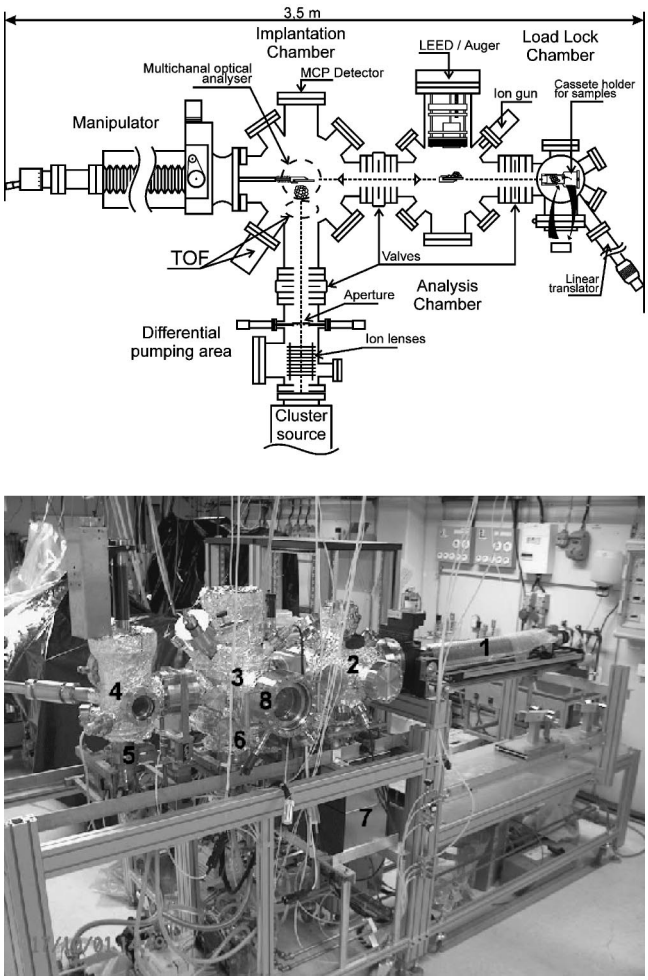

FIG. 1. Schematic diagram and photograph of the CIDA: (1) manipulator; (2) implantation chamber; (3) analysis chamber; (4) load-lock chamber; (5) and (6) turbomolecular pumps; (7) ion pump; and (8) LEED/Auger spectrometer.

In the present article we introduce a new ultrahigh vacuum (UHV) cluster implantation and deposition apparatus (CIDA) supplied by a pulsed cluster source (PUCLUS) from gaseous precursors. The apparatus has been constructed in the Atomic Physics Group of Gothenburg University and Chalmers University of Technology. The apparatus is designed to explore the above-mentioned potential applications of clusters produced from gaseous precursors and to provide more fundamental information concerning the cluster–surface interactions. Test experiments on beam control and first results on surface impact of clusters formed from gaseous precursors are reported.

II. EXPERIMENTAL SETUP

A. Cluster implantation and deposition apparatus (CIDA)

A schematic diagram and a photograph of the CIDA are shown in Fig. 1. The apparatus consists of implantation, analysis, load-lock, connection chambers, and manipulator. The implantation chamber is supplied with an ion pump (320 l/s), the other chambers with turbomolecular pumps (from 70 to 500 l/s) backed by rotary vane pumps. The chambers are separated by pneumatic UHV gate valves with leak rate $<1\times10^{-10}$ Torr l s^{-1}. The electronic control unit governs valve operation on vacuum lines, ensuring chamber isolation and manipulator protection against destruction by valve closing in the case of power failure. All chambers are supplied by heating tapes and covered with aluminum foil to get baking temperatures up to 200 °C. The pressure is measured by ion gauges.

The implantation chamber is spherical in shape with 16 ports from CF40 to CF160 in size. It is designed to study cluster surface collisions, deposition of thin films by cluster assembling, and provide shallow implantation of ionized clusters. For this reason UHV conditions up to 1×10^{-10} Torr are required and reached using the ion pump. The implantation chamber contains a multichannel plate (MCP) ion detector mounted on a CF100 flange to detect the cluster ion beam and a sapphire window (on a CF63 flange) for detection of light emission using an inductively coupled charge device camera with spectrograph. In addition, there are a time-of-flight (TOF) ion mass spectrometer and a quadrupole mass spectrometer that can be attached to the implantation chamber to detect both sputtered atoms from the bombarded substrate and scattered cluster fragments. The laboratory is situated next to the group laser laboratory which allows a range of *in situ* laser diagnostic techniques to be used (e.g., laser induced fluorescence and/or ionization of sputtered particles or backscattered cluster constituents, second harmonic generation on the target surface, etc.). Laser beams can be introduced to the chamber via two quartz windows mounted on CF40 flanges. All the above-described techniques provide a possibility of carrying out *in situ* measurements. Experiments in a controlled gas atmosphere are also possible by using a gas valve mounted on one of CF40 flanges. A manipulator is attached to the implantation chamber on a CF160 flange. This manipulator gives the possibility of exchanging samples from the special cassette holder in the load-lock chamber, to move the samples from chamber to chamber (total distance is up to 1 m), to change the geometry of the experiment (rotating and tilting of a holder with sample with respect to the cluster beam), and to vary the temperature of the substrate from liquid nitrogen temperature to 900 °C.

An analysis chamber is attached to the implantation chamber. This chamber is cylindrical (around the vertical axis) with 17 ports from CF40 to CF160 in size and evacuated by a 500 l/s turbomolecular pump. A low energy electron diffraction (LEED)/Auger spectrometer mounted on the side CF160 flange is for surface analysis. The spectrometer is supplied with an Ar ion gun with ion energy up to 5 keV. The ion gun can be used to clean a substrate surface before cluster implantation or deposition and to sputter the surface layers for investigation of samples modified by implantation. The chamber also contains CF40 ports with quartz windows allowing the use of laser diagnostics.

The load-lock chamber is cylindrical (around the vertical axis). It is evacuated by a small turbomolecular pump (70 l/s). A translator is mounted on the top of the chamber. Inside the chamber, this translator consists of four shelves for sample holders. Holders are loaded on the shelves by hand

through the fast load-lock door when the chamber is isolated from the rest of the apparatus by the valve. One more translator mounted from the side allows the operator to pick up a holder with the proper sample from the shelf and transfer it to the manipulator arm when it is in an extended position, i.e., in the load-lock chamber, and with all chambers pumped out.

The connection chamber between the cluster source and the implantation chamber is cylindrical (around the horizontal axis). It is used for final beam control (ion lenses, deflectors, and apertures), steering of the cluster beam into the implantation chamber, and also for differential pumping, i.e., elimination of a pressure difference between the high vacuum (10^{-7} Torr) of the PUCLUS, namely an acceleration chamber (see below) and the above-mentioned UHV of the implantation chamber. For that reason the relatively small volume connection chamber is evacuated by a 500 l/s turbomolecular pump.

B. Pulsed cluster source from gaseous precursors (PUCLUS)

A PUCLUS from gaseous precursors compatible with the CIDA has been developed (see Fig. 2). This is an assembly consisting of separately pumped chambers, namely an acceleration chamber and a source chamber containing a pulsed gas valve. Both chambers are evacuated by a large turbomolecular pump (1100 l/s). The pump is connected to the acceleration chamber using an adapter with two additional KF40 ports providing the pumping of the source chamber through flexible metal hoses.

The source chamber is responsible for cluster beam production and ionization. The chamber consist of a pulsed valve and a translator making it possible to adjust the position of the nozzle in all three dimensions relative to the skimmer. The skimmer is cone shaped with orifice of 1.9 mm and mounted on the inside cylinder separating the pumping area of the source chamber and acceleration chamber. The source chamber can be placed either in line with the acceleration chamber using a CF100 flange (No. 4 in Fig. 2) or, if desired, can be mounted on the other CF100 flange at a 90° angle to the main axis of the acceleration chamber as it is shown in Fig. 2. Either of those two configurations can be used, depending on the experimental task.

The pulsed valve for cluster production from gas phase precursors (Even-Lavie-5-2000 type obtained from Tel Aviv University) is mounted on a KF100 flange and attached to the source chamber. It is a solenoid type valve with the considerable advantage of producing very short pulses (10–15 μs) compared to other commercial systems, thus reducing the pumping requirements and allowing UHV conditions to be easily reached after differential pumping stages. The valve has a hardened stainless steel conical nozzle with an orifice diameter of 0.25 mm. Typical valve operating conditions produce a mean pressure in the source chamber between 8×10^{-5} and 2×10^{-4} Torr. It also works at very high gas stagnation pressure (up to 100 bar) that is advantageous for producing large clusters. The ionizer, made as a circular tungsten filament, is mounted on the same flange as the valve

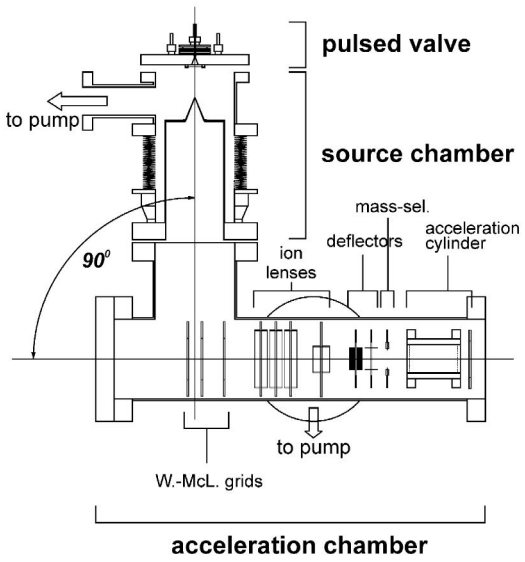

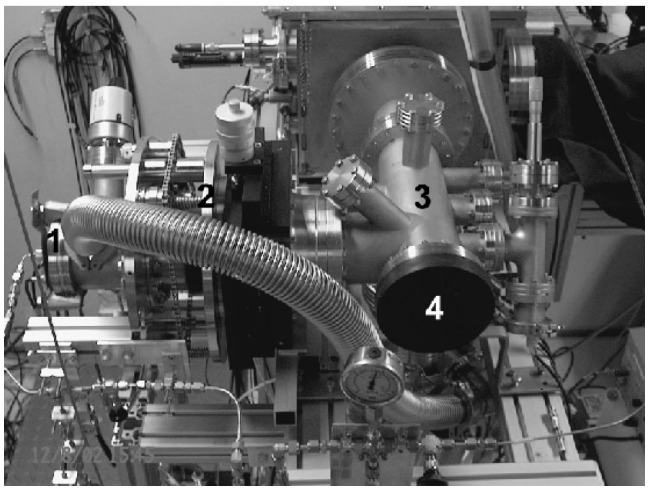

FIG. 2. Scheme and photograph of the PUCLUS: (1) pulsed valve; (2) source chamber with translator; (3) acceleration chamber; and (4) CF100 flange to place the source chamber in line with the acceleration one.

allowing ionization directly after cluster formation. A bias voltage of -60 to -120 V is typically applied and a thermionic emission current of a few mA was found to be sufficient for cluster ionization.

The next chamber holds all the parts needed for focusing, deflecting, and acceleration of the cluster ions. The preacceleration is achieved from the first three grids in a Wiley–McLaren configuration[19] used as part of a TOF mass spectrometer. The distance between the first two extraction grids is 15 mm with 25 mm between the last two grids. The pulsed voltages typically applied on grids one and two range from 1.5 to 4.5 kV, depending on desired experimental parameters, and the third grid remains grounded. At the next stage the beam is focused using a set of ion lenses with various diameters and different voltages applied to them. For beam deflection two pairs of deflectors, one for horizontal the other for vertical manipulation, were placed after each other. Apart from having a focused and deflected beam, the possibility of selecting clusters with a certain mass is provided. The principle of mass selection used is a gate, which is closed by a high voltage (a few keV). This voltage is

always applied apart from a very small controlled time (below 1 μs) when it opens to let the clusters with desired size pass through. In order to adjust the cluster implantation energy, a second acceleration stage is built. A cylinder closed on both ends by grids was mounted in the beam path and followed by a grounded grid. When the selected clusters are in the cylinder a high voltage pulse up to 20 kV is applied to the cylinder. The clusters are then accelerated to ground when they leave the cylinder. Hence, a total cluster energy of up to 25 keV can be reached after two acceleration stages. The pressure in the acceleration chamber is typically kept below 1×10^{-6} Torr.

For preliminary testing, the PUCLUS was connected to a temporary collision chamber supplied by a mechanical feedthrough with a sample holder and containing a MCP detector for cluster beam characterization. The three grids in a Wiley–McLaren configuration (described in the paragraph about the acceleration chamber) together with the MCP detector serve as a TOF mass spectrometer. A high resolution TOF analyzer/multiscaler (FAST Comtech) provides effective measuring conditions and supplies the raw data to a PC for further data processing.

III. EXPERIMENTAL RESULTS AND DISCUSSION

A. Cluster ion beam control

Gaseous nitrogen, oxygen, and argon were used for the first test experiments. First, the $X-Y$ position of the nozzle with respect to the skimmer was adjusted to optimize the cluster intensity and collimate the beam. The optimum nozzle–skimmer distance for maximum cluster intensity was found experimentally to lie between 20 and 25 mm. It is well known that the gas stagnation pressure influences the clustering process.[20] A comparison of different stagnation pressures was performed and as expected, the production of heavy-mass clusters benefits from higher pressure. The optimal stagnation pressure for the gases used here was 60–100 bar, depending on gas species. Due to the voltage applied to the ionizer, mounted directly after the region of gas expansion and clustering, the difference in potential between the ionizer and the grounded valve body provides a field that accelerates the cluster cloud on the way to the main acceleration grids. There is clearly a different distribution of masses at the different positions of the cloud when it arrives at the acceleration region. This is found by varying the time delay between the gas pulse and the acceleration pulse applied to the Wiley–McLaren grids that cuts out certain parts of the cluster ion cloud. Depending on which gas is used, the time-delay parameter window changes significantly.

Typical mass spectra of the clusters formed from various precursors at the gas stagnation pressure of 90 bar and a working pressure of 1.5×10^{-4} Torr in the source chamber are shown in Fig. 3. For nitrogen and oxygen [see Figs. 3(a) and 3(b)] the formation of mainly molecular clusters, i.e., with an even number of atoms is observed. Maximum cluster size is up to 150 atoms for Ar and 60–70 molecules for the molecular gases. For oxygen we also observe the presence of $(O_2)_n+H_2O$ clusters. Those clusters are probably formed due to water vapor trace contamination of the stainless steel

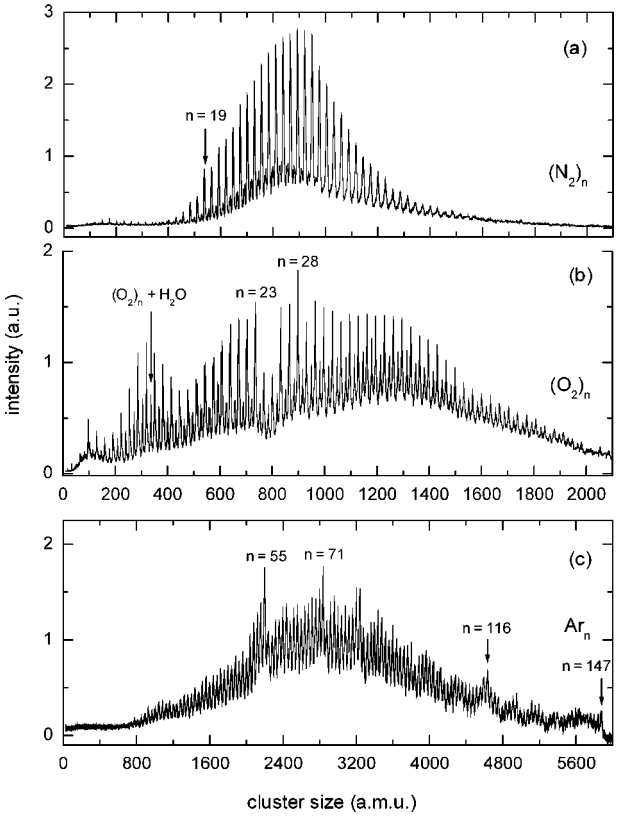

FIG. 3. Typical mass spectra for clusters of (a) nitrogen, (b) oxygen, and (c) argon; *n*: number of molecules of N and O and atoms for Ar in cluster. Details on the parameters of beam formation are in the text.

pipes supplying gas to the valve. Oxygen and nitrogen clusters proved to be particularly sensitive to the ionization energy, and if the thermionic emission current was set too high no clusters with more than ~5 molecules were found. This is probably due to fragmentation of heavier clusters.

When analyzing the cluster mass spectra one can find some strong mass peaks, often called magic numbers. These numbers correspond to geometrically filled cluster shells for van der Waals bound clusters and have a higher relative stability. The magic numbers vary for different cluster species; the reason for this is not yet always clearly understood, especially for molecular clusters, i.e., $(O_2)_n$ and $(N_2)_n$ in the present case. In the case of Ar the magic numbers found are the same as those observed earlier for noble gases, in particular for xenon, and described in terms of icosahedral symmetry.[21]

B. Cluster surface collisions and hillock formation

Samples of glass covered with 100 nm thick ITO films and pyrolytic graphite were used as targets for cluster–surface collision experiments. The samples were bombarded by $(O_2)_n^+$ and Ar_n^+ clusters with various *n* values and energies of 14–15 keV/cluster. The impact angle was varied from normal to the surface to 45°. The surfaces were then analyzed by the atomic force microscopy (AFM) technique. The machine used was a Dimension 3000 from Digital Instruments, and run in the tapping mode.

When a surface is bombarded by energetic clusters one might expect craters to appear on the surface,[22] but AFM

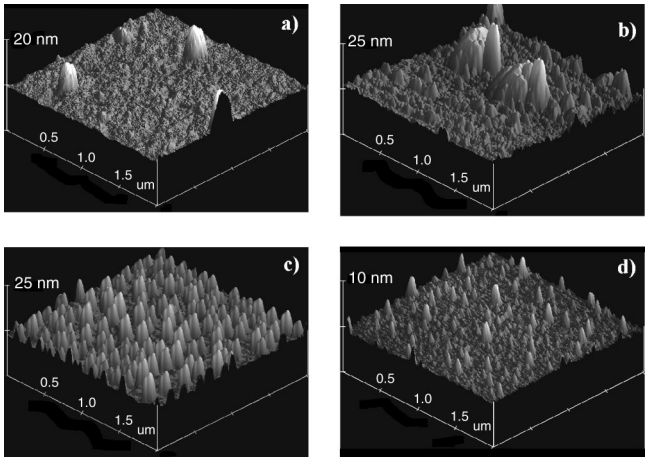

FIG. 4. AFM images of: (a) ITO bombarded by 14 keV Ar_{70-80} clusters at normal impact angle (single collisions); (b) ITO bombarded by 14 keV Ar_{90-100} clusters at 45° impact angle (single collisions); (c) ITO bombarded by 15 keV $(O_2)_{30-40}$ clusters at 45° impact angle (dose 10^7-10^8 cluster/cm^2); and (d) graphite bombarded by 15 keV $(O_2)_{30-40}$ clusters at normal impact angle (dose 10^7 cluster/cm^2).

pictures showed that nanosize hillocks had formed. Hillock formation is a well known phenomenon for MeV-energy cluster implantation, for example.[23,24] This effect is considered as promising for electron emission device fabrication.[25,26] Only recently a similar hillock formation was found on a Si surface under 40–60 keV CO_2 cluster implantation,[17,18] but the nature of this effect is not clearly understood yet.

In Fig. 4(a) one can see hillocks formed on the ITO surface bombarded by 14 keV Ar^+_{70-80} clusters at normal impact angle. Those hillocks are structures consisting of protruding substrate material. They are between cylindrical and conical in shape with a height of 10–15 nm. The base diameter is about 150–250 nm. Tilting the substrate to give a 45° impact angle has a dramatic effect on the hillocks. The AFM image in Fig. 4(b) shows clear multihillock formation. The clusters in this case were large, up to 100 atoms, and the multihillock structures are thought to have been created by either multicollision effects or by fragmentation of the cluster upon impact into smaller units, causing several very local hillocks. When the implantation dose (time of sample exposure to the cluster beam) is increased and the cluster species changed to oxygen, hillocks quite uniform in shape and size are formed on the bombarded area [Fig. 4(c)]. The substrate material also plays an important role in the hillock formation. Figure 4(d) shows a graphite surface bombarded with oxygen clusters under similar experimental conditions to the ITO case, shown in Fig. 4(c). One can see that the hillocks on the graphite become smaller and the size distribution is wider compared to the ITO sample.

Hillock formation could be caused by heat transferred to the surface upon cluster collision. While the implantation depth of the clusters is very shallow (a few nm), the heat transferred reaches a much bigger volume, melting the surface at the collision spot. Hillock formation would probably originate from the elastic rebound of the lattice and thermal expansion of the melted material which is pushed away from the surface forming the protruding structures. Parameters influencing the hillock formation are, naturally, the cluster ion beam characteristics such as cluster species, size, energy, and dose and impact angle. Substrate parameters such as the melting point and density probably play an important role too. From comparison of Figs. 4(c) and 4(d) one can see that the denser ITO (7.14 g/cm^3) with a lower melting point (2200 K) compared to pyrolytic graphite (2.25 g/cm^3, ~4000 K) provides more prominent hillock formation. The study of the hillocks' dependence on the implantation conditions and type of substrate will be continued.

ACKNOWLEDGMENTS

The authors acknowledge financial support from the Göran Gustafsson Foundation for Research in Natural Science and Medicine, Sweden and The Swedish Research Council, Vetenskapsrådet.

[1] P. Milani and S. Iannotta, *Cluster Beam Synhtesis of Nanostructured Materials* (Springer, Berlin, 1999).
[2] T. Takagi, Mater. Sci. Eng., A **253**, 30 (1998).
[3] W. A. De Heer, Rev. Mod. Phys. **65**, 611 (1993).
[4] *Clusters of Atoms and Molecules*, edited by H. Haberland (Springer, Berlin, 1994).
[5] E. E. B. Campbell and I. V. Hertel, Nucl. Instrum. Methods Phys. Res. B **112**, 48 (1996).
[6] A. V. Glotov and E. E. B. Campbell, Phys. Rev. A **62**, 033202 (2000).
[7] E. E. B. Campbell and F. Rohmund, Rep. Prog. Phys. **63**, 1061 (2000).
[8] T. Takagi, I. Yamada, and A. Sasaki, Thin Solid Films **39**, 207 (1976).
[9] I. Yamada and J. Matsuo, Mater. Res. Soc. Symp. Proc. **427**, 265 (1996).
[10] I. Yamada and J. Matsuo, Mater. Sci. Semicond. Process. **1**, 27 (1998).
[11] R. D. Levine, in *The Physics and Chemistry of Clusters*, edited by E. E. B. Campbell and M. Larsson (World Scientific, Singapore, 2001), p. 110.
[12] M. Togo, K. Noda, and T. Tanigawa, Tech. Dig. - Int. Electron Devices Meet. 347 (1998).
[13] J. O. Borland, Semicond. Int. **4**, (2001).
[14] M. Akizuki, J. Matsuo, I. Yamada, M. Harada, S. Ogasawara, and A. Doi, Nucl. Instrum. Methods Phys. Res. B **112**, 83 (1996).
[15] S. A. Klopcic and M. F. Jarrold, J. Chem. Phys. **106**, 8855 (1997).
[16] J. Matsuo, E. Minami, M. Saito, N. Toyoda, H. Katsumata, and I. Yamada, Eur. Phys. J. D **9**, 635 (1999).
[17] J.-H. Song, S. N. Kwon, D.-K. Choi, and W.-K. Choi, Nucl. Instrum. Methods Phys. Res. B **179**, 568 (2001).
[18] J.-H. Song and W.-K. Choi, Nucl. Instrum. Methods Phys. Res. B **190**, 792 (2002).
[19] W. C. Wiley and I. H. McLaren, Rev. Sci. Instrum. **26**, 1150 (1955).
[20] O. F. Hagena, Surf. Sci. **106**, 101 (1981).
[21] W. Miehle, O. Kandler, T. Leisner, and O. Echt, J. Chem. Phys. **91**, 5940 (1989).
[22] I. Yamada, J. Matsuo, Z. Insepov, T. Aoki, T. Seki, and N. Toyoda, Nucl. Instrum. Methods Phys. Res. B **164–165**, 944 (2000).
[23] S. M. M. Ramos, N. Bonardi, B. Canut, S. Bouffard, and S. Della-Negra, Nucl. Instrum. Methods Phys. Res. B **143**, 319 (1998).
[24] M. Döbeli, F. Ames, C. R. Musil, L. Scandella, M. Suter, and H. A. Synal, Nucl. Instrum. Methods Phys. Res. B **143**, 503 (1998).
[25] P. Thevenard, J. P. Dupin, V. T. Binh, S. T. Purcell, V. Semet, and D. Guillot, Nucl. Instrum. Methods Phys. Res. B **166–167**, 788 (2000).
[26] P. Thevenard, J. P. Dupin, B. V. Thien, S. T. Purcell, and V. Semet, Surf. Coat. Technol. **128–129**, 59 (2000).